Generalized hyper-Ramsey resonance with separated oscillating fields

T. Zanon-Willette*
LERMA, Observatoire de Paris, PSL Research University, CNRS, Sorbonne Universités, UPMC Université Paris 06, F-75005 Paris, France

V. I. Yudin and A. V. Taichenachev
Institute of Laser Physics, Siberian Branch of Russian Academy of Sciences, Novosibirsk 630090, Russia;
Novosibirsk State University, Novosibirsk 630090, Russia;
and Novosibirsk State Technical University, Novosibirsk 630092, Russia

(Received 11 March 2015; published 14 August 2015)

An exact generalization of the Ramsey transition probability is derived to improve ultrahigh precision measurement and quantum state engineering when a particle is subjected to independently-tailored separated oscillating fields. The phase shift accumulated at the end of the interrogation scheme and associated with the particle wave function is offering a very high-level control of quantum states throughout various laser parameters conditions. The generalized hyper-Ramsey resonance based on independent manipulation of interaction time, field amplitude, phase, and frequency detuning is presented to increase performances in the next generation of atomic, molecular, and nuclear clocks, to upgrade high-resolution frequency measurement in Penning trap mass spectrometry and for a better control of light-induced frequency shifts in matter-wave interferometer or quantum information processing.

DOI: 10.1103/PhysRevA.92.023416 PACS number(s): 32.80.Qk, 06.20.Jr, 32.70.Jz

I. INTRODUCTION

Precision measurement plays a critical role in many fields of physics such as metrology and fundamental tests of physical theories. Laser pulsed spectroscopy is one technique to achieve such measurements. It is now a universal tool to investigate interaction between light and matter in quantum clocks [1–5], in cavity quantum electrodynamics experiments [6–8], and in atomic, molecular, and neutron interferometry [9–11].

To improve the resolution of frequency measurements in the atomic and molecular beam resonance method initially invented by Rabi *et al.* [12], Ramsey proposed to replace the single oscillatory field with a double microwave excitation pulse separated by a free evolution without any electromagnetic-field perturbation [13,14].

The low sensitivity of Ramsey's spectroscopy to field inhomogeneities associated with a strong reduction of light shift on the probing atomic transition has drastically impacted the time and frequency metrology [15–17], leading to microwave standards at the relative 10^{-16} level of accuracy [18,19].

Ultrahigh resolution of frequency measurement has been achieved with very long storage times of Doppler and recoil free quantum particles using laser cooling techniques in ion traps [1,20] and optical lattice clocks [21,22]. The level of 10^{-18} relative accuracy, almost achieved [23], requires a very precise control of atomic or molecular interactions to cancel systematic frequency shifts whether fermionic or bosonic species are used [24,25]. With the next generation of quantum clocks, stringent tests of general relativity would be accessible, as well as new applications in geophysics and hydrology [26]. Also more recently, very high-precision measurement has become relevant for mass spectrometry [27], where the highest precision was reached using ions in a Penning trap. The use of Ramsey's method of separated oscillating fields has provided a significant reduction in the uncertainty of the cyclotron frequency and thus of the ion mass of interest combined with a faster acquisition rate [28–30].

For the next level of progress in very high precision, the recent hyper-Ramsey scheme [31–33] is a promising evolution of Ramsey pulsed spectroscopy that overcomes some issues. Composite pulses inspired by nuclear magnetic resonance techniques [34] are now used to compensate simultaneously for noise decoherence, pulse area fluctuation, and residual frequency offset due to the applied laser field itself. The first or the second pulse of the usual Ramsey sequence can be separated into two or more contiguous sections which lead to probing protocols with more degrees of freedom in order to minimize resonance shifts [35,36]. It is also reminiscent of the spin-echo technique, where the sequence of pulses was originally applied to suppress inhomogeneous effects, causing a spin relaxation [37,38]. The hyper-Ramsey method was successfully implemented on a single trapped $^{171}Yb^{+}$ ion demonstrating efficient reduction of the light shift by several orders of magnitude [39].

II. GENERALIZED VERSION OF THE RAMSEY TRANSITION PROBABILITY

We have established an accurate generalization of the Ramsey interrogation for transition probability. This formalism provides a practical guide to the design, implementation, and interpretation of pulse sequences, and it is thus of considerable importance for high-precision spectroscopy widely used in fundamental and applied physics. The resonance can be coherently excited by weakly allowed transitions [22], stimulated two-photon Raman transitions [40–42], by magnetically induced transitions [43], or by quadrupolar radio-frequency field interaction in mass spectrometry [44]. It produces an accurate control of energy levels at the end of the interrogation sequence.

*thomas.zanon@upmc.fr

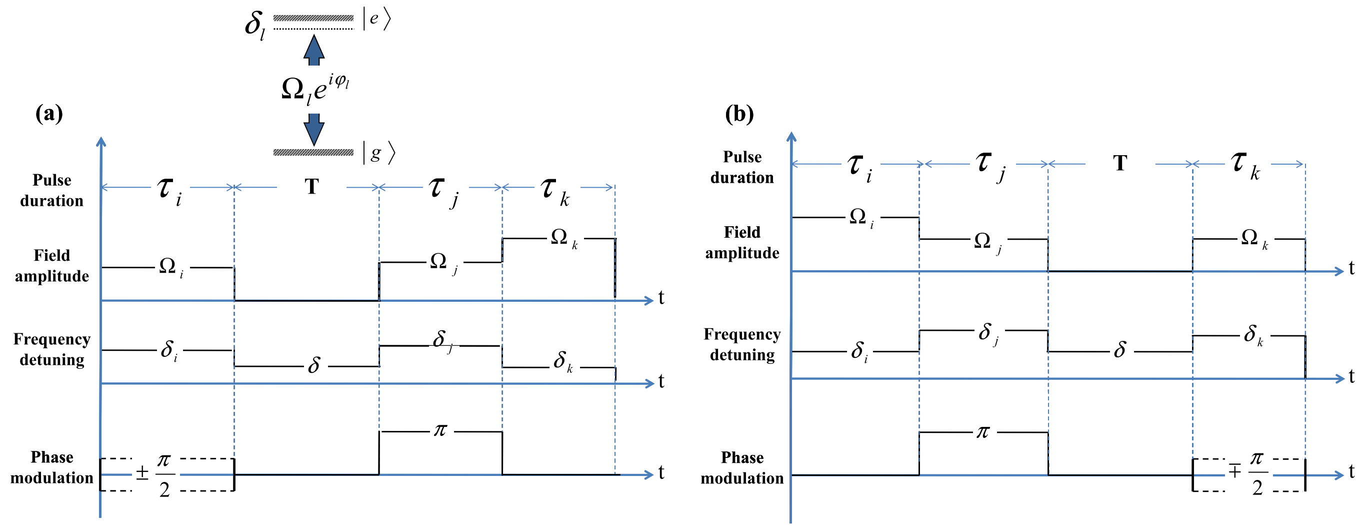

FIG. 1. (Color online) Quantum system with a narrow $|g\rangle \leftrightarrow |e\rangle$ clock transition probed by a laser pulse excitation. (a) Sequence of composite pulses $\theta_i,\delta T,\theta_j,\theta_k$ and (b) $\theta_i,\theta_j,\delta T,\theta_k$, with specified laser parameters including detuning δ_l, complex field amplitude $\Omega_l e^{i\varphi_l}$, pulse duration τ_l, where $l = i,j,k$, and a free evolution time T between pulses. A phase step modulation of the appropriate laser field φ_l may be applied in both schemes if necessary.

A. Analytical form of the transition probability

Adopting a multizone interaction wave-function model [40], we have derived the analytical form of the generalized transition probability and the phase shift driving the resonance frequency position around the extremum of the fringe. This derivation extends the work in Ref. [31]. The generalized transition probability is derived for independent particles interacting with separated and controllable oscillating fields. Field amplitudes, frequency detunings, and pulse durations can be manipulated individually within two different probing schemes, shown in Figs. 1(a) and 1(b). The sequence of composite pulses described by the analytical expression of the transition probability is investigated to improve control of external perturbations such as light-shifts or residual magnetic fields on the line shape [45,46]. It can be implemented in trapped atom clocks and extended to ion-trap mass spectrometers and molecular beams or fountain devices where moving particles are interacting with multiple oscillating fields during a free fly.

The generalized transition probability must be dependent on pulse area $\theta_l = \omega_l \tau_l/2$ $(l = i,j,k)$ with different driving Rabi amplitudes Ω_l and frequency detunings δ_l via the generalized Rabi frequency $\omega_l = \sqrt{\delta_l^2 + \Omega_l^2}$. During the pulses, light-shift from off-resonant states may be present and a laser step frequency utilized to rectify the anticipated shift, thus requiring a redefinition of frequency detunings as $\delta_l \equiv \delta_l \pm \Delta_l$. Additional phase inversion of laser fields and nonuniform pulsed excitation conditions modifying the entire spectral line shape are included into the computation of the transition [31,47]. The exact expression of the generalized Ramsey probability for a particle starting from initial state $|g\rangle$ to final state $|e\rangle$ is given in a compact form as

$$P_{|g\rangle\mapsto|e\rangle} = \alpha[1+\beta(\Phi)^2]\left[1+\frac{2\beta(\Phi)}{1+\beta(\Phi)^2}\cos(\delta T + \Phi)\right], \quad (1)$$

with a clock frequency detuning δ during free evolution without light. We have introduced for convenience the notation

$$\beta(\Phi) = \beta\sqrt{1+\tan^2\Phi}, \quad (2)$$

where envelopes α,β driving the resonance amplitude are respectively defined by

$$\alpha = \left(1+\frac{\delta_i^2}{\omega_i^2}\tan^2\theta_i\right)\left(1+\frac{\delta_{jk}^2}{\omega_{jk}^2}\tan^2\theta_{jk}\right)\left(\frac{\Omega_j}{\omega_j}\tan\theta_j+\frac{\Omega_k}{\omega_k}\tan\theta_k\right)^2\cos^2\theta_i\cos^2\theta_j\cos^2\theta_k, \quad (3a)$$

$$\beta = \frac{\frac{\Omega_i}{\omega_i}\tan\theta_i\left(1-\frac{\delta_j\delta_k+\Omega_j\Omega_k}{\omega_j\omega_k}\tan\theta_j\tan\theta_k\right)}{\left(1-\frac{\delta_i\delta_{jk}}{\omega_i\omega_{jk}}\tan\theta_i\tan\theta_{jk}\right)\left(\frac{\Omega_j}{\omega_j}\tan\theta_j+\frac{\Omega_k}{\omega_k}\tan\theta_k\right)}\,\frac{1-\frac{\frac{\delta_j}{\omega_j}\tan\theta_j+\frac{\delta_k}{\omega_k}\tan\theta_k}{1-\frac{\delta_j\delta_k+\Omega_j\Omega_k}{\omega_j\omega_k}\tan\theta_j\tan\theta_k}\,\frac{\frac{\delta_i}{\omega_i}\tan\theta_i+\frac{\delta_{jk}}{\omega_{jk}}\tan\theta_{jk}}{1-\frac{\delta_i\delta_{jk}}{\omega_i\omega_{jk}}\tan\theta_i\tan\theta_{jk}}}{1+\left(\frac{\frac{\delta_i}{\omega_i}\tan\theta_i+\frac{\delta_{jk}}{\omega_{jk}}\tan\theta_{jk}}{1-\frac{\delta_i\delta_{jk}}{\omega_i\omega_{jk}}\tan\theta_i\tan\theta_{jk}}\right)^2}, \quad (3b)$$

including a reduced variable,

$$\frac{\delta_{jk}}{\omega_{jk}}\tan\theta_{jk} = \frac{(\delta_j\Omega_k-\Omega_j\delta_k)\tan\theta_j\tan\theta_k}{\Omega_j\omega_k\tan\theta_j+\Omega_k\omega_j\tan\theta_k}. \quad (4)$$

The phase shift accumulated after the entire interrogation scheme is

$$\tan\Phi = \frac{\dfrac{\frac{\delta_j}{\omega_j}\tan\theta_j + \frac{\delta_k}{\omega_k}\tan\theta_k}{1-\frac{\delta_j\delta_k+\Omega_j\Omega_k}{\omega_j\omega_k}\tan\theta_j\tan\theta_k} + \dfrac{\frac{\delta_i}{\omega_i}\tan\theta_i + \frac{\delta_{jk}}{\omega_{jk}}\tan\theta_{jk}}{1-\frac{\delta_i\delta_{jk}}{\omega_i\omega_{jk}}\tan\theta_i\tan\theta_{jk}}}{1 - \dfrac{\frac{\delta_j}{\omega_j}\tan\theta_j + \frac{\delta_k}{\omega_k}\tan\theta_k}{1-\frac{\delta_j\delta_k+\Omega_j\Omega_k}{\omega_j\omega_k}\tan\theta_j\tan\theta_k}\,\dfrac{\frac{\delta_i}{\omega_i}\tan\theta_i + \frac{\delta_{jk}}{\omega_{jk}}\tan\theta_{jk}}{1-\frac{\delta_i\delta_{jk}}{\omega_i\omega_{jk}}\tan\theta_i\tan\theta_{jk}}}. \quad (5)$$

From Eqs. (1) to (5), lineshape, population transfer efficiency and frequency shift affecting the resonance can be used to accurately evaluate various experimental laser pulse conditions including Rabi excitation, Ramsey and Hyper-Ramsey schemes [12,13,31]. Note that a second composite sequence of pulses can be realized as proposed in Fig. 1(b). All previous expressions are still valid by simply exchanging subscripts $i \rightleftarrows k$ with corresponding laser parameters while reversing the sign for pulse durations $\tau_l \mapsto -\tau_l$ and free evolution time $T \mapsto -T$. We have checked the consistency of the results by adopting a rotating coordinate system to obtain numerical expressions for transition probabilities in various configurations of laser parameters [48–52] in parallel with a wave-function model [40,53,54].

To highlight a natural connection between the well-known method of separated oscillatory fields by Ramsey [13–15] and the generalized formalism presented in this work, in the Appendix we report a straightforward derivation of the standard Ramsey transition probability based on our generalized pulse sequence.

B. Generalized expression of the phase-shift

The phase shift given by Eq. (5) is the primary result needed in precise control of quantum states to suppress any frequency shift induced by the laser excitation itself. By tailoring phase-shift parameters and engineering the resonance amplitude, it is possible to generate quantum spectroscopy signals for increased resolution or better stability. Following [55], Eq. (5) can be written into a closed-form solution as

$$\Phi = \arctan\left[\frac{\frac{\delta_j}{\omega_j}\tan\theta_j + \frac{\delta_k}{\omega_k}\tan\theta_k}{1-\left(\frac{\delta_j\delta_k+\Omega_j\Omega_k}{\omega_j\omega_k}\right)\tan\theta_j\tan\theta_k}\right] + \arctan\left[\frac{\delta_{jk}}{\omega_{jk}}\tan\theta_{jk}\right] + \arctan\left[\frac{\delta_i}{\omega_i}\tan\theta_i\right]. \quad (6)$$

It is thus feasible to eliminate the frequency shift of the central fringe by engineering Eq. (6) with particular choices of laser step frequency, pulse duration, and phase inversion to achieve a desired interference minimum. The key point is to establish some efficient quantum control protocols which compensate for frequency shift and are robust to small changes in pulse area while achieving a highly contrasted population transfer between the targeted states [36]. Such quantum engineering of phase shift has been recently proposed in a generalized hyper-Raman-Ramsey spectroscopy of a stimulated two-photon forbidden clock transition of strontium ^{88}Sr and ytterbium ^{174}Yb, eliminating the detrimental light-shift contribution [40].

The generalized hyper-Ramsey transition probability has been computed with some pulse protocols reported in Table I. The standard sequence referring to the Ramsey (R) protocol is compared with two others sequences based on nonstandard G-H-R protocols. The panels of Fig. 2 display resonance fringes corresponding to selected protocols in

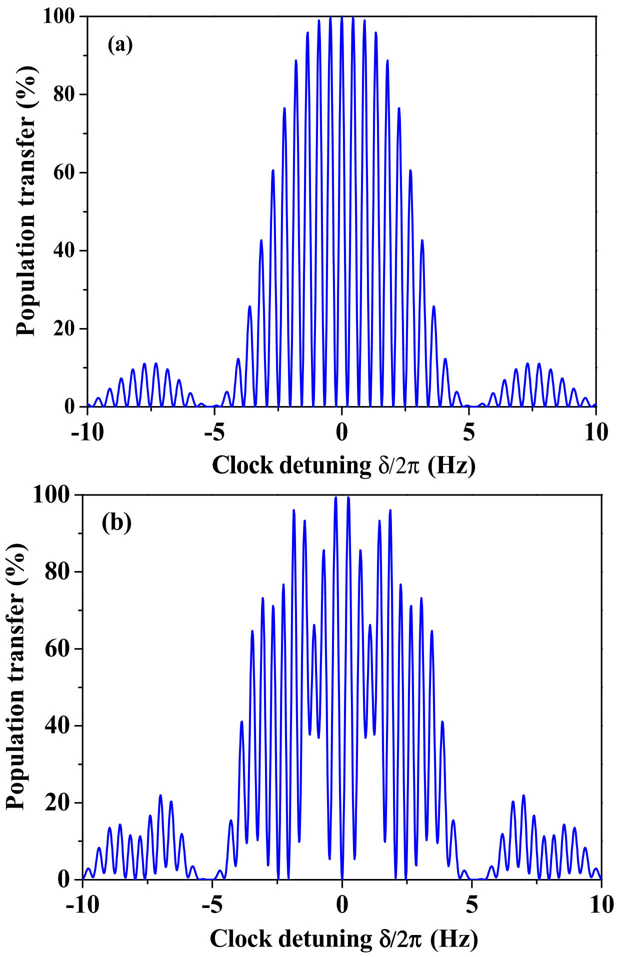

FIG. 2. (Color online) Generalized hyper-Ramsey resonances $P_{|g\rangle\mapsto|e\rangle}$ versus the clock detuning δ computed from Eqs. (1) to (5). (a) Ramsey resonance. (b) Hyper-Ramsey resonance from all G-H-R protocols reported in Table I. The optimal Rabi frequency of the laser field is defined as $\Omega = \pi/2\tau$. Pulse duration is $\tau = 0.1875$ s with a free evolution time $T = 2$ s and $\Delta_l = 0$ $(l = i,j,k)$.

TABLE I. Selected Ramsey (R) and generalized hyper-Ramsey (G-H-R) pulse protocols shown in Figs. 1(a) and 1(b), where $\Delta_l = 0$ $(l = i,j,k)$. The Rabi frequency of the light field is defined as $\Omega = \pi/2\tau$ and possible phase inversion of the light field during a pulse is indicated. The phase step modulation of the laser field is off.

Protocols	Parameters	θ_i	θ_j	θ_k
	τ_l	τ	0	τ
R	Ω_l	Ω	0	Ω
	δ_l	δ	0	δ
	τ_l	τ	2τ	τ
	Ω_l	$\pm\Omega$	$\mp\Omega$	$\pm\Omega$
G-H-R	δ_l	δ	δ	δ
	τ_l	τ	τ	τ
	Ω_l	$\pm\Omega$	$\mp 2\Omega$	$\pm\Omega$
	δ_l	δ	2δ	δ

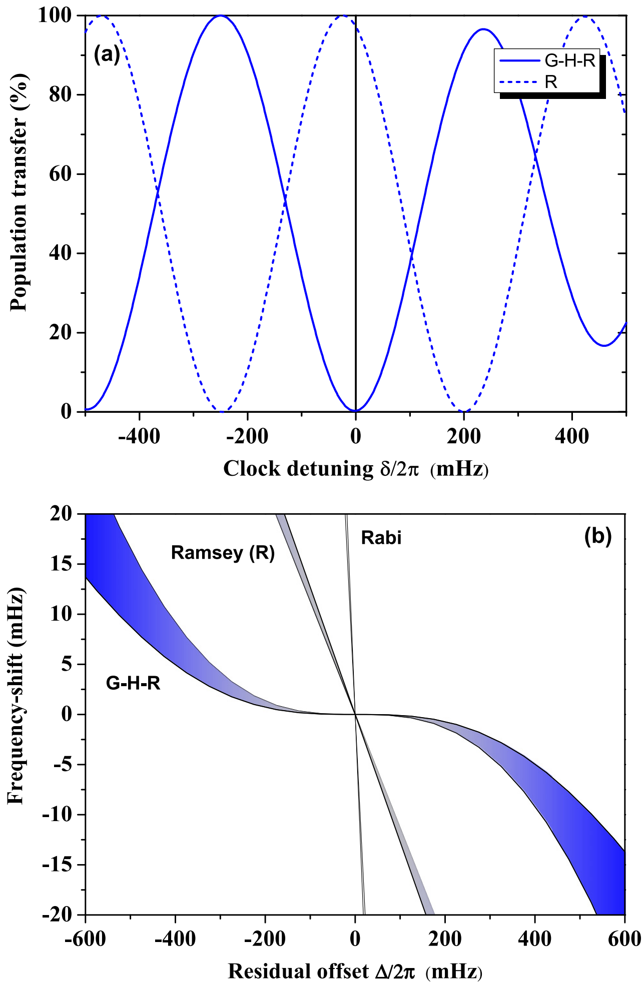

FIG. 3. (Color online) (a) Small offset fixed around $\Delta/2\pi \sim$ 220 mHz inducing a frequency shift on the central Ramsey resonance (dashed line) and the generalized hyper-Ramsey resonance (solid line). (b) Central fringe frequency shift $-\Phi/2\pi T$ based on Eq. (5) [Eq. (6)] as a function of the residual offset $\delta \equiv \Delta$ for all protocols reported in Table I. All curves are also shown with a $\pm 10\%$ pulse area variation (shadow areas between solid lines). Others parameters are identical to those of Fig. 2.

Table I. In Fig. 2(a), Ramsey fringes have been simulated using parameters following the R protocol with two $\theta_i = \theta_k = \pi/2$ pulse areas. Hyper-Ramsey fringes have also been simulated with $\theta_i = \pi/2$ and $\theta_j = \pi, \theta_k = \pi/2$ pulse areas according to G-H-R protocols, leading to the same resonance line shown in Fig. 2(b).

Nonlinear behaviors of the central fringe frequency shift versus a small frequency perturbation in the clock detuning have been investigated and presented in Figs. 3(a) and 3(b). The curves are compared to the linear frequency shift resulting from a single Rabi pulse excitation to help guide the eye. Figure 3(a) shows the effect of a small external frequency offset on the central fringe position. In contrast to the normal Ramsey spectroscopy, the generalized hyper-Ramsey resonance method provides a vastly reduced sensitivity of the central fringe's frequency shift to external perturbations. As evidenced in Fig. 3(b), small perturbations such as the residual light shift or magnetic-field fluctuations may manifest themselves as laser frequency steps during the spectroscopy pulse sequence, but the central fringe position has a very flat slope for its frequency shift dependence, which is more than one order of magnitude smaller than that for Ramsey. The combination of $\theta_i = \pi/2$ and $\theta_j = \pi, \theta_k = \pi/2$ pulse areas in Eq. (6) compensates for all terms over a large residual error in frequency, as well as their first- and second-order sensitivity to frequency fluctuation. The suppression of the central fringe shift may be finally made insensitive to small pulse area variation by inserting an intermediate "echo" pulse with a sign inversion of the light field only during the intermediate $\theta_j = -\pi$ pulse or during the initial and final $\theta_i = \theta_k = -\pi/2$ pulses (see Table I). Simultaneously, a laser frequency step may be ultimately applied during pulses to compensate for any frequency offset larger than the width of the resonance.

C. Phase step modulation of the resonance

The top plot in Fig. 3(a) raises a serious concern for precision metrology. While the minimum of the Ramsey fringe

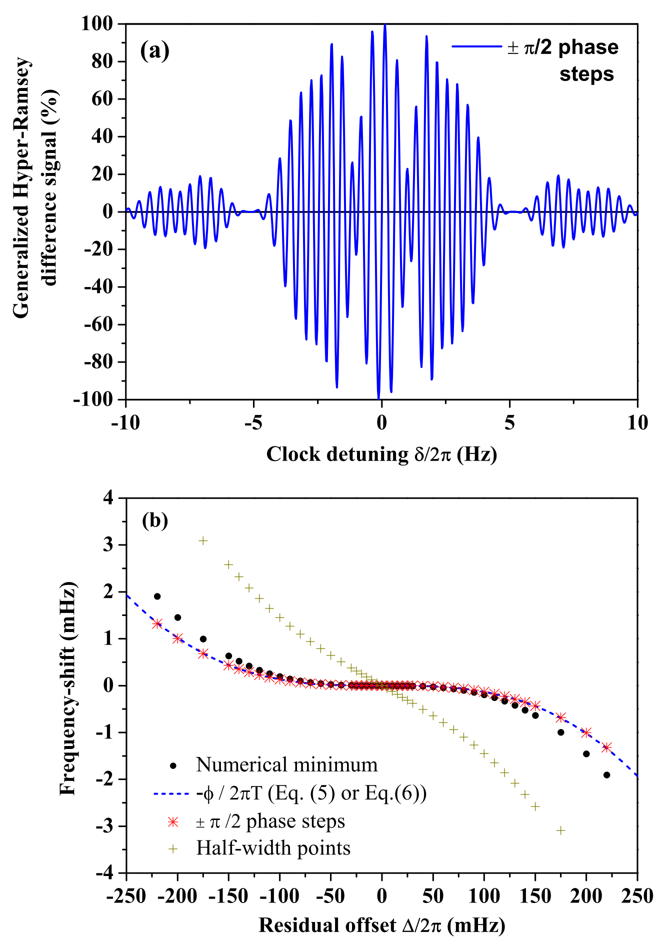

FIG. 4. (Color online) (a) Dispersive error signal generated by a $\pm\pi/2$ phase step modulation of appropriate laser fields. (b) Evaluation of the frequency shift versus a residual frequency offset by a numerical tracking of the central fringe extremum (solid black dots), by the phase step process of Eq. (1) (solid stars), by an evaluation based on Eq. (5) [Eq. (6)] with $-\Phi/2\pi T$ (dashed line), or by probing the central fringe at half-width points (solid crosses).

occurs at the line center, the first maxima of the G-H-R fringes on either side differ in amplitude by 3%–4%. Many precision experiments, as clock experiments, actually lock to the central feature to stabilize the frequency on the line center. Since locking requires an odd symmetry feature, the exciting laser usually has its frequency modulated to generate the needed signal. However, modulation of an asymmetric resonance would lead to off-center locking, exactly what we are trying to avoid with the G-H-R technique. The amount of shift depends on the modulation details, but a typical modulation usually at half width of the central fringe is required. If the 50% population levels are not equally spaced from the line center, the resulting modulated line will be slightly pulled out from line center.

In order to eliminate the asymmetry effect on the true position of the central fringe, we propose to apply a $\pm\pi/2$ phase step modulation of the cosine function in Eq. (1) as in Refs. [56,57]. The effect of the laser phase modulation on the transition probability is discussed in the Appendix with a complex wave-function model. Figure 4(a) shows the resulting dispersive error signal generated in this way. Figure 4(b) presents a comparison between different frequency-locking techniques to probe the extremum of the central fringe. Solid black dots report the exact position of the extremum by a numerical tracking of Eq. (1). By applying a frequency modulation technique and probing the interferences at the half-width points to lock to the center of the resonance, the slight asymmetry of the line shape reintroduces a weak linear dependance of the frequency shift with a residual frequency offset. Even in the presence of a weak line-shape asymmetry, the phase step modulation of Eq. (1) is able to reproduce very well the frequency shift based on Eq. (5) [Eq. (6)]. This phase modulation technique directly produces an error signal with enhanced immunity to residual offset fluctuations [39,57,58].

III. CONCLUSION

In conclusion, the generalized hyper-Ramsey resonance provides a new performing tool much required for the next generation of quantum interferometers sensitive to very small laser parameters fluctuations. Although the initial Ramsey's method of separated oscillating fields has proven to be very useful in fundamental and applied physics based on laser pulsed spectroscopy, it still has some fundamental limitations. To overcome these issues, a nonstandard generalization of the Ramsey protocol has been considered and demonstrated to be even more successful 65 yr after the original scheme was proposed. The hyper-Ramsey spectral resonance has been fully extended in this paper to include potential biases, higher-order light-shift corrections on detunings, and various modifications of laser parameters exploring nonlinear frequency responses of quantum particles for ultraprecise frequency measurement.

The application of the generalized hyper-Ramsey resonance should be able to strongly improve frequency uncertainty measurements in subsequent tests of fundamental physics based on atomic or molecular fountains [59–61], in charged ions [62,63], for small changes in molecular vibrational frequencies based on clocks sensitive to potential variation in the electron-to-proton mass ratio [64,65], and in searching for a weak parity violation in chiral molecules by laser spectroscopy [66]. Quantum phase-shift engineering should impact high-resolution mass spectrometry based on the application of the Ramsey method to short-lived ions stored in Penning traps [29] and laser pulsed spectroscopy in cold-molecule chemistry [67,68]. Using the generalized hyper-Ramsey spectroscopy for Stark decelerated cold molecules may allow a significant improvement of the frequency measurement uncertainty, which can be important for the search of the time variation of the fine structure constant [69], in measuring gravitationally induced quantum phase shifts for neutrons [70], and for observing spin-dependent nuclear scattering lengths of neutrons in Ramsey interferometers [71]. In the future, a pair of stretched hyperfine states from a ^{229}Th nuclear transition may provide a large suppression of several external field shifts [72,73], where an ultranarrow clock transition will offer an exquisite test of nuclear quantum engineering spectroscopy at the next level of 10^{-19} relative accuracy.

ACKNOWLEDGMENTS

T.Z.-W. deeply acknowledges C. Janssen for checking calculations and J. Ye, E. Arimondo, J. Dalibard, B. Darquié, M. Glass-Maujean, M. Minissale, R. Metzdorff, A.D. Ludlow, E. de Clercq, M-L. Dubernet-Tuckey, and Y. Té for discussions and a careful reading of the manuscript. V.I.Yu. and A.V.T. were supported by the RFBR (Grants No. 14-02-00712, No. 14-02-00939, and No. 14-02-00806), by the Russian Academy of Sciences, by Presidium of the Siberian Branch of the Russian Academy of Sciences, by the RF Ministry of Education and Science (State Assignment No. 2014/139,Project No. 825).

APPENDIX

1. Wave-function model including phase of the laser field

We present the wave-function formalism [13,40,53] to establish Eqs. (1) to (5) in the main section of the paper. It is based on a two-level system describing the superposition of the $|g\rangle,|e\rangle$ clock states as

$$|\Psi(\theta_l)\rangle = c_g(\theta_l)|g\rangle + c_e(\theta_l)|e\rangle, \tag{A1}$$

where the pulse area is defined by $\theta_l = \omega_l\tau_l/2$ and the effective Rabi field is $\omega_l^2 = \delta_l^2 + \Omega_l^2$. Using the solution of the Schrödinger's equation, we write for the $c_{g,e}(\theta_l)$ $(l = i,j,k)$ transition amplitudes

$$\begin{pmatrix} c_g(\theta_l) \\ c_e(\theta_l) \end{pmatrix} = \chi(\theta_l)M(\theta_l)\begin{pmatrix} c_g(0) \\ c_e(0) \end{pmatrix}, \tag{A2}$$

including a phase factor of the form $\chi(\theta_l) = \exp[-i\delta_l\frac{\tau_l}{2}]$. The wave-function evolution driven by the pulse area θ_l is determined by a complex 2×2 spinor interaction matrix [48–50,54],

$$\begin{aligned} M(\theta_l) &= \begin{pmatrix} M_+(\theta_l) & e^{\imath\varphi_l}M_\dagger(\theta_l) \\ e^{-\imath\varphi_l}M_\dagger(\theta_l) & M_-(\theta_l) \end{pmatrix} \\ &= \begin{pmatrix} \cos(\theta_l) + i\frac{\delta_l}{\omega_l}\sin(\theta_l) & -ie^{i\varphi_l}\frac{\Omega_l}{\omega_l}\sin(\theta_l) \\ -ie^{-i\varphi_l}\frac{\Omega_l}{\omega_l}\sin(\theta_l) & \cos(\theta_l) - i\frac{\delta_l}{\omega_l}\sin(\theta_l) \end{pmatrix}, \end{aligned} \tag{A3}$$

where the phase of the laser field is introduced by φ_l. The pulsed excitation is written as a product of different matrices

$M(\theta_l)$ and a free evolution without laser light during a time T. Generalized hyper-Ramsey expression for respective composite sequences $\theta_i,\delta T,\theta_j,\theta_k$ and $\theta_i,\theta_j,\delta T,\theta_k$, which depend on initials conditions $c_g(0)$ and $c_e(0)$, are

$$\begin{pmatrix} c_g(\theta_i,\delta T,\theta_j,\theta_k) \\ c_e(\theta_i,\delta T,\theta_j,\theta_k) \end{pmatrix} = \chi(\theta_i,\theta_j,\theta_k) \begin{pmatrix} M_+(\theta_i)M_+(\theta_j,\theta_k) & M_\dagger(\theta_i)e^{i\varphi_i}M_+(\theta_j,\theta_k) \\ +M_\dagger(\theta_j,\theta_k)M_\dagger(\theta_i)e^{[-i(\delta T+\varphi_i)]} & +M_\dagger(\theta_j,\theta_k)M_-(\theta_i)e^{[-i\delta T]} \\ M_\dagger(\theta_k,\theta_j)M_+(\theta_i) & M_\dagger(\theta_k,\theta_j)M_\dagger(\theta_i)e^{i\varphi_i} \\ +M_\dagger(\theta_i)M_-(\theta_j,\theta_k)e^{[-i(\delta T+\varphi_i)]} & +M_-(\theta_j,\theta_k)M_-(\theta_i)e^{[-i\delta T]} \end{pmatrix} \begin{pmatrix} c_g(0) \\ c_e(0) \end{pmatrix}, \tag{A4}$$

$$\begin{pmatrix} c_g(\theta_i,\theta_j,\delta T,\theta_k) \\ c_e(\theta_i,\theta_j,\delta T,\theta_k) \end{pmatrix} = \chi(\theta_i,\theta_j,\theta_k) \begin{pmatrix} M_+(\theta_k)M_+(\theta_i,\theta_j) & M_\dagger(\theta_j,\theta_i)M_+(\theta_k) \\ +M_\dagger(\theta_i,\theta_j)M_\dagger(\theta_k)e^{[-i(\delta T-\varphi_k)]} & +M_\dagger(\theta_k)M_-(\theta_i,\theta_j)e^{[-i(\delta T-\varphi_k)]} \\ M_\dagger(\theta_k)e^{-i\varphi_k}M_+(\theta_i,\theta_j) & M_\dagger(\theta_j,\theta_i)M_\dagger(\theta_k)e^{-i\varphi_k} \\ +M_\dagger(\theta_i,\theta_j)M_-(\theta_k)e^{[-i\delta T]} & +M_-(\theta_i,\theta_j)M_-(\theta_k)e^{[-i\delta T]} \end{pmatrix} \begin{pmatrix} c_g(0) \\ c_e(0) \end{pmatrix}, \tag{A5}$$

with $\chi(\theta_i,\theta_j,\theta_k)=\chi(\theta_i)\chi(\theta_j)\chi(\theta_k)$ and where reduced matrix components are

$$\begin{aligned} M_+(\theta_j,\theta_k) &= M_+(\theta_j)M_+(\theta_k)+M_\dagger(\theta_j)M_\dagger(\theta_k)e^{-i(\varphi_j-\varphi_k)}, \\ M_-(\theta_j,\theta_k) &= M_-(\theta_j)M_-(\theta_k)+M_\dagger(\theta_j)M_\dagger(\theta_k)e^{i(\varphi_j-\varphi_k)}, \\ M_\dagger(\theta_j,\theta_k) &= M_\dagger(\theta_j)e^{i\varphi_j}M_+(\theta_k)+M_\dagger(\theta_k)e^{i\varphi_k}M_-(\theta_j), \\ M_\dagger(\theta_k,\theta_j) &= M_\dagger(\theta_k)e^{-i\varphi_k}M_+(\theta_j)+M_\dagger(\theta_j)e^{-i\varphi_j}M_-(\theta_k), \end{aligned} \tag{A6}$$

$$\begin{aligned} M_+(\theta_i,\theta_j) &= M_+(\theta_i)M_+(\theta_j)+M_\dagger(\theta_i)M_\dagger(\theta_j)e^{-i(\varphi_i-\varphi_j)}, \\ M_-(\theta_i,\theta_j) &= M_-(\theta_i)M_-(\theta_j)+M_\dagger(\theta_i)M_\dagger(\theta_j)e^{i(\varphi_i-\varphi_j)}, \\ M_\dagger(\theta_i,\theta_j) &= M_\dagger(\theta_j)e^{-i\varphi_j}M_+(\theta_i)+M_\dagger(\theta_i)e^{-i\varphi_i}M_-(\theta_j), \\ M_\dagger(\theta_j,\theta_i) &= M_\dagger(\theta_i)e^{i\varphi_i}M_+(\theta_j)+M_\dagger(\theta_j)e^{i\varphi_j}M_-(\theta_i). \end{aligned} \tag{A7}$$

The final expression is an hyper-Ramsey complex amplitude. We are now able to make explicit the transition probability $P_{|g\rangle\mapsto|e\rangle}$ for the two composite sequences.

For the first composite sequence $\theta_i,\delta T,\theta_j,\theta_k$ shown in Fig. 1(a), we have

$$P_{|g\rangle\mapsto|e\rangle} = c_e(\theta_i,T,\theta_j,\theta_k)c_e^*(\theta_i,T,\theta_j,\theta_k), \tag{A8a}$$

$$= |\alpha|^2|1+\beta e^{-i(\delta T-\Phi+\varphi_i)}|^2, \tag{A8b}$$

where wave-function envelopes α,β driving the resonance amplitude are

$$\alpha = [M_+(\theta_i)c_g(0)+M_\dagger(\theta_i)e^{i\varphi_i}c_e(0)]M_\dagger(\theta_k,\theta_j)\chi(\theta_i,\theta_j,\theta_k), \tag{A9a}$$

$$\beta e^{i\Phi} = \left[\frac{M_\dagger(\theta_i)c_g(0)+M_-(\theta_i)c_e(0)}{M_+(\theta_i)c_g(0)+M_\dagger(\theta_i)e^{i\varphi_i}c_e(0)}\right]\frac{M_-(\theta_j,\theta_k)}{M_\dagger(\theta_k,\theta_j)}. \tag{A9b}$$

For the second composite sequence $\theta_i,\theta_j,\delta T,\theta_k$ shown in Fig. 1(b), we also have

$$P_{|g\rangle\mapsto|e\rangle} = c_e(\theta_i,\theta_j,T,\theta_k)c_e^*(\theta_i,\theta_j,T,\theta_k), \tag{A10a}$$

$$= |\alpha|^2|1+\beta e^{-i(\delta T-\Phi-\varphi_k)}|^2, \tag{A10b}$$

where envelopes α,β driving the resonance amplitude are now

$$\alpha = [M_+(\theta_i,\theta_j)c_g(0)+M_\dagger(\theta_j,\theta_i)c_e(0)]M_\dagger(\theta_k)e^{-i\varphi_k} \times\chi(\theta_i,\theta_j,\theta_k), \tag{A11a}$$

$$\beta e^{i\Phi} = \left[\frac{M_\dagger(\theta_i,\theta_j)c_g(0)+M_-(\theta_i,\theta_j)c_e(0)}{M_+(\theta_i,\theta_j)c_g(0)+M_\dagger(\theta_j,\theta_i)c_e(0)}\right]\frac{M_-(\theta_k)}{M_\dagger(\theta_k)}. \tag{A11b}$$

In all cases, the phase term Φ represents the atomic phase shift accumulated by the wave function during the laser interrogation sequence. Starting from an initial condition $c_g(0)=1$ and $c_e(0)=0$, phase-shift expressions for sequences presented in Figs. 1(a) and 1(b) are respectively given by

$$\Phi = \mathrm{Arg}\left[\frac{M_\dagger(\theta_i)}{M_+(\theta_i)}\frac{M_-(\theta_j,\theta_k)}{M_\dagger(\theta_k,\theta_j)}\right], \tag{A12a}$$

$$\Phi = \mathrm{Arg}\left[\frac{M_\dagger(\theta_i,\theta_j)}{M_+(\theta_i,\theta_j)}\frac{M_-(\theta_k)}{M_\dagger(\theta_k)}\right]. \tag{A12b}$$

When phases of laser fields are ignored in Eqs. (A6) and (A7), these expressions lead to the analytical form given by Eq. (5). It determines the clock frequency shift measured on the central fringe in a generalized hyper-Ramsey spectroscopy. Note that by applying a specific phase modulation of the laser field with $\varphi_i=\pm\pi/2,\varphi_j=\pi,\varphi_k=0$ $[\varphi_i=0,\varphi_j=\pi,\varphi_k=\mp\pi/2]$ in Eqs. (A4), (A6), (A8b) [Eqs. (A5), (A7), (A10b)], then subtracting both components with opposite sign, we obtain the dispersive curve reported in Fig. 4(a).

2. Ramsey transition probability $(\theta,\delta T,\theta)$

We derive the analytical expression for the standard Ramsey transition probability from the generalized expression established in the main section. We plug into in Eqs. (1) to (5) the values for the Ramsey case from Table I with $\theta_j=0$ and $\theta_i=\theta_k=\theta$, where Eq. (2) is reduced to 1 and Eq. (4) is 0. The generalized transition probability from state $|g\rangle$ to state

$|e\rangle$ takes the form

$$P_{|g\rangle\mapsto|e\rangle} = 2\frac{\Omega^2}{\omega^2}\sin^2\theta\left(\cos^2\theta + \frac{\delta^2}{\omega^2}\sin^2\theta\right)[1+\cos(\delta T + \Phi)], \tag{A13}$$

where the Ramsey phase shift is found to be [55]

$$\Phi = \arctan\left[\frac{2\frac{\delta}{\omega}\tan\theta}{1-\left(\frac{\delta}{\omega}\right)^2\tan^2\theta}\right] = 2\arctan\left[\frac{\delta}{\omega}\tan\theta\right]. \tag{A14}$$

By applying a trigonometrical transformation on

$$\begin{aligned}\left(\cos^2\theta + \frac{\delta^2}{\omega^2}\sin^2\theta\right)\times[1+\cos(\delta T+\Phi)] &= 2\left[\frac{\cos\theta + i\frac{\delta}{\omega}\sin\theta}{2}e^{i\frac{\delta T}{2}} + \frac{\cos\theta - i\frac{\delta}{\omega}\sin\theta}{2}e^{-i\frac{\delta T}{2}}\right]^2\\ &= 2\left[\cos\left(\frac{\delta T}{2}\right)\cos\theta - \frac{\delta}{\omega}\sin\left(\frac{\delta T}{2}\right)\sin\theta\right]^2,\end{aligned} \tag{A15}$$

we recover the standard expression of the transition probability derived by Ramsey in 1950 for a spin-$\frac{1}{2}$ interacting with a radio-frequency field [13,14] as

$$P_{|g\rangle\mapsto|e\rangle} = 4\frac{\Omega^2}{\omega^2}\sin^2\theta\left[\cos\left(\frac{\delta T}{2}\right)\cos\theta - \frac{\delta}{\omega}\sin\left(\frac{\delta T}{2}\right)\sin\theta\right]^2, \tag{A16}$$

where $\theta = \omega\tau/2$.

---

[1] T. Rosenband, D. B. Hume, P. O. Schmidt, C. W. Chou, A. Brusch, L. Lorini, W. H. Oskay, R. E. Drullinger, T. M. Fortier, J. E. Stalnaker, S. A. Diddams, W. C. Swann, N. R. Newbury, W. M. Itano, D. J. Wineland, and J. C. Bergquist, Frequency ratio of Al^+ and Hg^+ single-ion optical clocks; Metrology at the 17th Decimal place, Science **319**, 1808 (2008).

[2] D. J. Wineland, Nobel Lecture: Superposition, entanglement, and raising Schrödinger's cat, Rev. Mod. Phys. **85**, 1103 (2013).

[3] N. Hinkley, J. A. Sherman, N. B. Phillips, M. Schioppo, N. D. Lemke, K. Beloy, M. Pizzocaro, C. W. Oates, and A. D. Ludlow, An atomic clock with 10^{-18} instability , Science **341**, 1215 (2013).

[4] B. J. Bloom, T. L. Nicholson, J. R. Williams, S. L. Campbell, M. Bishof, X. Zhang, W. Zhang, S. L. Bromley, and J. Ye, An optical lattice clock with accuracy and stability at the 10^{-18} level, Nature (London) **506**, 71 (2014).

[5] R. Le Targat, L. Lorini, Y. Le Coq, M. Zawada, J. Guéna, M. Abgrall, M. Gurov, P. Rosenbusch, D. G. Rovera, B. Nagórny, R. Gartman, P. G. Westergaard, M. E. Tobar, M. Lours, G. Santarelli, A. Clairon, S. Bize, P. Laurent, P. Lemonde, and J. Lodewyck, Experimental realization of an optical second with strontium lattice clocks, Nat. Commun. **4**, 2109 (2013).

[6] M. Brune, S. Haroche, V. Lefevre, J. M. Raimond, and N. Zagury, Quantum nondemolition measurement of small photon numbers by Rydberg-atom phase-sensitive detection, Phys. Rev. Lett. **65**, 976 (1990).

[7] S. Gleyzes, S. Kuhr, C. Guerlin, J. Bernu, S. Deléglise, U. Busk Hoff, M. Brune, J.-M. Raimond, and S. Haroche, Quantum jumps of light recording the birth and death of a photon in a cavity, Nature (London) **446**, 297 (2007).

[8] S. Haroche, Nobel Lecture: Controlling photons in a box and exploring the quantum to classical boundary, Rev. Mod. Phys. **85**, 1083 (2013).

[9] A. D. Cronin, J. Schmiedmayer, and D. E. Pritchard, Optics and interferometry with atoms and molecules, Rev. Mod. Phys. **81**, 1051 (2009).

[10] P. R. Berman, *Atom interferometry* (Academic Press, San Diego, CA, 1996).

[11] J. Klepp, S. Sponar, and Y. Hasegawa, Fundamental phenomena of quantum mechanics explored with neutron interferometers, Prog. Theor. Exp. Phys. (2014) 082A01.

[12] I. I. Rabi, J. R. Zacharias, S. Millman, and P. Kusch, A new method of measuring nuclear magnetic moment, Phys. Rev. **53**, 318 (1938).

[13] N. F. Ramsey, A molecular beam resonance method with separated oscillating fields, Phys. Rev. **78**, 695 (1950).

[14] N. F. Ramsey, *Molecular beams* (Clarendon Press, Oxford, 1956).

[15] N. F. Ramsey, Experiments with separated oscillatory fields and hydrogen masers, Rev. Mod. Phys. **62**, 541 (1990).

[16] J. Vanier and C. Audoin, *The Quantum Physics of Atomic Frequency Standards* (Adam Hilger IOP, Bristol, U.K., 1989).

[17] K. Gibble and S. Chu, Future Slow-atom Frequency Standards, Metrologia **29**, 201 (1992).

[18] R. Wynands and S. Weyers, Atomic fountain clocks, Metrologia **42**, S64 (2005).

[19] S. Bize, P. Laurent, M. Abgrall, H. Marion, I. Maksimovic, L. Cacciapuoti, J. Grünert, C. Vian, F. Pereira dos Santos, P. Rosenbusch, P. Lemonde, G. Santarelli, P. Wolf, A. Clairon, A. Luiten, M. Tobar, and C. Salomon, Cold atom clocks and applications, J. Phys. B **38**, S449 (2005).

[20] H. S. Margolis, Trapped ion optical clocks, Eur. Phys. J. Spec. Top. **172**, 97 (2009).

[21] A. Derevianko and H. Katori, *Colloquium*: Physics of optical lattice clocks, Rev. Mod. Phys. **83**, 331 (2011).

[22] A. D. Ludlow, M. M. Boyd, J. Ye, E. Peik, and P. O. Schmidt, Optical atomic clocks, Rev. Mod. Phys. **87**, 637 (2015).
[23] T. L. Nicholson, S. L. Campbell, R. B. Hutson, G. E. Marti, B. J. Bloom, R. L. McNally, W. Zhang, M. D. Barrett, M. S. Safronova, G. F. Strouse, W. L. Tew, and J. Ye, Systematic evaluation of an atomic clock at 2×10^{-18} total uncertainty, Nat. Commun. **6**, 6896 (2015).
[24] G. K. Campbell, M. M. Boyd, J. W. Thomsen, M. J. Martin, S. Blatt, M. D. Swallows, T. L. Nicholson, T. Fortier, C. W. Oates, S. A. Diddams, N. D. Lemke, P. Naidon, P. Julienne, J. Ye, and A. D. Ludlow, Probing interactions between ultracold fermions, Science **324**, 360 (2009).
[25] C. Lisdat, J. S. R. Vellore Winfred, T. Middelmann, F. Riehle, and U. Sterr, Collisional losses, decoherence, and frequency shifts in optical lattice clocks with bosons, Phys. Rev. Lett. **103**, 090801 (2009).
[26] C. W. Chou, D. B. Hume, T. Rosenband, and D. J. Wineland, Optical clocks and relativity, Science **329**, 1630 (2010).
[27] K. Blaum, High-accuracy mass spectrometry with stored ions, Phys. Rep. **425**, 1 (2006).
[28] G. Bollen, H.-J. Kluge, T. Otto, G. Savard, and H. Stolzenberg, Ramsey technique applied in a Penning trap mass spectrometer, Nucl. Instrum. Methods Phys. Res., Sect. B **70**, 490 (1992).
[29] S. George, S. Baruah, B. Blank, K. Blaum, M. Breitenfeldt, U. Hager, F. Herfurth, A. Herlert, A. Kellerbauer, H.-J. Kluge, M. Kretzschmar, D. Lunney, R. Savreux, S. Schwarz, L. Schweikhard, and C. Yazidjian, Ramsey method of separated oscillatory fields for high-precision Penning trap mass spectrometry, Phys. Rev. Lett. **98**, 162501 (2007).
[30] M. Eibach, T. Beyer, K. Blaum, M. Block, K. Eberhardt, F. Herfurth, J. Ketelaer, Sz. Nagy, D. Neidherr, W. Nörtershäuser, and C. Smorra, First investigation of phase-shifted Ramsey excitation in Penning trap mass spectrometry, Int. J. Mass Spectrom. **303**, 27 (2011).
[31] V. I. Yudin, A. V. Taichenachev, C. W. Oates, Z. W. Barber, N. D. Lemke, A. D. Ludlow, U. Sterr, Ch. Lisdat, and F. Riehle, Hyper-Ramsey spectroscopy of optical clock transitions, Phys. Rev. A **82**, 011804(R) (2010).
[32] K. S. Tabatchikova, A. V. Taichenachev, and V. I. Yudin, Generalized ramsey scheme for precision spectroscopy of ultracold atoms and ions: Inclusion of a finite laser line width and spontaneous relaxation of the atomic levels, JETP Lett. **97**, 311 (2013).
[33] K. S. Tabatchikova, A. V. Taichenachev, A. K. Dmitriev, and V. I. Yudin, Study of field shifts of Ramsey resonances on ultracold atoms and ions, JETP Lett. **120**, 203 (2015).
[34] M. H. Levitt, Composite pulses, Prog. Nucl. Magn. Reson. Spectrosc. **18**, 61 (1986).
[35] L. M. K. Vandersypen and I. L. Chuang, NMR techniques for quantum control and computation, Rev. Mod. Phys. **76**, 1037 (2005).
[36] M. Braun and S. J. Glaser, Concurrently optimized cooperative pulses in robust quantum control: Application to broadband Ramsey-type pulse sequence elements , New J. Phys. **16**, 115002 (2014).
[37] E. L. Hahn, Spin Echoes, Phys. Rev. **80**, 580 (1950).
[38] H. Y. Carr, Steady-state free precession in nuclear magnetic resonance, Phys. Rev. **112**, 1693 (1958).
[39] N. Huntemann, B. Lipphardt, M. Okhapkin, Chr. Tamm, E. Peik, A. V. Taichenachev, and V. I. Yudin, Generalized Ramsey excitation scheme with suppressed light shift, Phys. Rev. Lett. **109**, 213002 (2012).
[40] T. Zanon-Willette, S. Almonacil, E. de Clercq, A. D. Ludlow, and E. Arimondo, Quantum engineering of atomic phase shifts in optical clocks, Phys. Rev. A **90**, 053427 (2014).
[41] M. Kasevich and S. Chu, Atomic interferometry using stimulated Raman transitions, Phys. Rev. Lett. **67**, 181 (1991).
[42] K. Moler, D. S. Weiss, M. Kasevich, and S. Chu, Theoretical analysis of velocity-selective Raman transitions, Phys. Rev. A **45**, 342 (1992).
[43] A. V. Taichenachev, V. I. Yudin, C. W. Oates, C. W. Hoyt, Z. W. Barber, and L. Hollberg, Magnetic field-induced spectroscopy of forbidden optical transitions with application to lattice-based optical atomic clocks, Phys. Rev. Lett. **96**, 083001 (2006); Z. W. Barber, C. W. Hoyt, C. W. Oates, L. Hollberg, A. V. Taichenachev, and V. I. Yudin, Direct excitation of the forbidden clock transition in neutral ^{174}Yb atoms confined to an optical lattice, *ibid.* **96**, 083002 (2006).
[44] M. Kretzschmar, The Ramsey method in high-precision mass spectrometry with Penning traps: Theoretical foundations, Int. J. Mass Spectrom. **264**, 122 (2007).
[45] J. H. Shirley, Some causes of resonant frequency shifts in atomic beam machines. I. shifts due to other frequencies of excitation, J. Appl. Phys. **34**, 783 (1963).
[46] G. L. Greene, Observation of the Bloch-Siegert effect in the Ramsey separated-oscillatory-field technique, Phys. Rev. A **18**, 1057 (1978).
[47] A. B. Brandin, Transition probability in the Ramsey method with arbitrary initial and final frequencies of separated oscillatory fields, Phys. Rev. A **50**, 1575 (1994).
[48] I. I. Rabi, N. F. Ramsey, and J. Schwinger, Use of rotating coordinates in magnetic resonance problems, Rev. Mod. Phys. **26**, 167 (1954).
[49] E. T. Jaynes, Matrix treatment of nuclear induction, Phys. Rev. **98**, 1099 (1955).
[50] H. Goldstein, *Classical Mechanics*, 2nd ed. (Addison-Wesley, Reading, MA, 1980).
[51] R. P. Feynman, F. L. Vernon, and R. W. Hellwarth, Geometrical Representation of the Schrodinger equation for solving maser problems, J. Appl. Phys. **28**, 49 (1957).
[52] M. Glass-Maujean and H. Henry Stroke, Rotating coordinates and the Ramsey separated oscillating-field resonance method, Am. J. Phys. **59**, 886 (1991).
[53] F. Bloch and I. I. Rabi, Atoms in variable magnetic fields, Rev. Mod. Phys. **17**, 237 (1945).
[54] D. A. Varshalovich, A. N. Moskalev, and V. K. Khersonskii, *Quantum Theory of Angular Momentum* (World Scientific, Singapore, 1988).
[55] M. Abramowitz and I. A. Stegun, *Handbook of Mathematical Functions* (Dover, New York, 1968).
[56] N. F. Ramsey and H. B. Silsbee, Phase shifts in the molecular beam method of separated oscillating fields, Phys. Rev. **84**, 506 (1951).
[57] V. Letchumanan, P. Gill, E. Riis, and A. G. Sinclair, Optical Ramsey spectroscopy of a single trapped $^{88}Sr^{+}$ ion, Phys. Rev. A **70**, 033419 (2004).
[58] A. Morinaga, F. Riehle, J. Ishikawa, and J. Helmcke, A Ca optical frequency standard: Frequency stabilization by means of nonlinear Ramsey resonances, Appl. Phys. B **48**, 165 (1989);

Optical frequency standards, IEEE Trans. Instrum. Meas. **38**, 524 (1989).
[59] R. G. Beausoleil and T. W. Hansch, Ultrahigh-resolution two-photon optical Ramsey spectroscopy of an atomic fountain, Phys. Rev. A **33**, 1661 (1986).
[60] H. L. Bethlem, M. Kajita, B. Sartakov, G. Meijer, and W. Ubachs, Prospects for precision measurements on ammonia molecules in a fountain, Eur. Phys. J. Spec. Top. **163**, 55 (2008).
[61] M. R. Tarbutt, B. E. Sauer, J. J. Hudson, and E. A. Hinds, Design for a fountain of YbF molecules to measure the electron's electric dipole moment, New J. Phys. **15**, 053034 (2013).
[62] M. S. Safronova, V. A. Dzuba, V. V. Flambaum, U. I. Safronova, S. G. Porsev, and M. G. Kozlov, Highly charged ions for atomic clocks, quantum information, and search for α variation, Phys. Rev. Lett. **113**, 030801 (2014).
[63] V. I. Yudin, A. V. Taichenachev, and A. Derevianko, Magnetic-dipole transitions in highly charged ions as a basis of ultraprecise optical clocks, Phys. Rev. Lett. **113**, 233003 (2014).
[64] A. Shelkovnikov, R. J. Butcher, C. Chardonnet, and A. Amy-Klein, Stability of the proton-to-electron mass ratio, Phys. Rev. Lett. **100**, 150801 (2008).
[65] S. Schiller, D. Bakalov, and V. I. Korobov, Simplest molecules as candidates for precise optical clocks, Phys. Rev. Lett. **113**, 023004 (2014).
[66] S. Tokunaga, S. C. Stoeffler, F. Auguste, A. Shelkovnikov, C. Daussy, A. Amy-Klein, C. Chardonnet, and B. Darquié, Probing weak force induced parity violation by high resolution mid-infrared molecular spectroscopy, Mol. Phys. **111**, 2363 (2013).
[67] S. Y. T. van de Meerakker, H. L. Bethlem, N. Vanhaecke, and G. Meijer, Manipulation and control of molecular beams, Chem. Rev. **112**, 4828 (2012).
[68] C. E. Heiner, D. Carty, G. Meijer, and H. L. Bethlem, A molecular synchrotron, Nat. Phys. **3**, 115 (2007).
[69] E. R. Hudson, H. J. Lewandowski, B. C. Sawyer, and J. Ye, Cold molecule spectroscopy for constraining the evolution of the fine structure constant, Phys. Rev. Lett. **96**, 143004 (2006).
[70] H. Abele, T. Jenke, H. Leeb, and J. Schmiedmayer, Ramsey's method of separated oscillating fields and its application to gravitationally induced quantum phase shifts, Phys. Rev. D **81**, 065019 (2010).
[71] F. M. Piegsa, B. van den Brandta, H. Glättlic, P. Hautlea, J. Kohlbrechera, J. A. Kontera, B. S. Schlimmed, and O. Zimmerb, A Ramsey apparatus for the measurement of the incoherent neutron scattering length of the deuteron, Nucl. Instrum. Methods Phys. Res., Sect. A **589**, 318 (2008).
[72] E. Peik and C. Tamm, Nuclear laser spectroscopy of the 3.5 eV transition in Th-229, Euro. Phys. Lett. **61**, 181 (2003).
[73] C. J. Campbell, A. G. Radnaev, A. Kuzmich, V. A. Dzuba, V. V. Flambaum, and A. Derevianko, Single-Ion Nuclear Clock for Metrology at the 19th Decimal Place, Phys. Rev. Lett. **108**, 120802 (2012).